ESC European Society of Cardiology

Cardiovascular Research (2017) **113**, 1560–1573
doi:10.1093/cvr/cvx161

Endothelial to haematopoietic transition contributes to pulmonary arterial hypertension

Olin D. Liang[1,2]*, Eui-Young So[1,2], Pamela C. Egan[1], Laura R. Goldberg[1], Jason M. Aliotta[3], Keith Q. Wu[2], Patrycja M. Dubielecka[1], Corey E. Ventetuolo[3], Anthony M. Reginato[4], Peter J. Quesenberry[1], and James R. Klinger[3]

[1]Division of Hematology/Oncology, Department of Medicine; [2]Center for Regenerative Medicine, Department of Orthopaedics; [3]Division of Pulmonary, Critical Care and Sleep Medicine, Department of Medicine; and [4]Division of Rheumatology, Department of Medicine, Rhode Island Hospital, Warren Alpert Medical School of Brown University, Providence, RI 02903, USA

Received 11 October 2016; revised 16 March 2017; editorial decision 9 August 2017; accepted 10 August 2017; online publish-ahead-of-print 7 September 2017

Time for primary review: 34 days

Aims The pathogenic mechanisms of pulmonary arterial hypertension (PAH) remain unclear, but involve dysfunctional endothelial cells (ECs), dysregulated immunity and inflammation in the lung. We hypothesize that a developmental process called endothelial to haematopoietic transition (EHT) contributes to the pathogenesis of pulmonary hypertension (PH). We sought to determine the role of EHT in mouse models of PH, to characterize specific cell types involved in this process, and to identify potential therapeutic targets to prevent disease progression.

Methods and results When transgenic mice with fluorescence protein ZsGreen-labelled ECs were treated with Sugen/hypoxia (Su/Hx) combination to induce PH, the percentage of ZsGreen+ haematopoietic cells in the peripheral blood, primarily of myeloid lineage, significantly increased. This occurrence coincided with the depletion of bone marrow (BM) ZsGreen+ c-kit+ CD45- endothelial progenitor cells (EPCs), which could be detected accumulating in the lung upon PH-induction. Quantitative RT-PCR based gene array analysis showed that key transcription factors driving haematopoiesis were expressed in these EPCs. When transplanted into lethally irradiated recipient mice, the BM-derived EPCs exhibited long-term engraftment and haematopoietic differentiation capability, indicating these EPCs are haemogenic in nature. Specific inhibition of the critical haematopoietic transcription factor Runx1 blocked the EHT process *in vivo*, prevented egress of the BM EPCs and ultimately attenuated PH progression in Su/Hx- as well as in monocrotaline-induced PH in mice. Thus, myeloid-skewed EHT promotes the development of PH and inhibition of this process prevents disease progression in mouse models of PH. Furthermore, high levels of Runx1 expression were found in circulating CD34+ CD133+ EPCs isolated from peripheral blood of patients with PH, supporting the clinical relevance of our proposed mechanism of EHT.

Conclusion EHT contributes to the pathogenesis of PAH. The transcription factor Runx1 may be a novel therapeutic target for the treatment of PAH.

Keywords Endothelial to haematopoietic transition • Endothelial progenitor cells • Transcription factor Runx1 • Haematopoiesis • Pulmonary arterial hypertension

1. Introduction

Pulmonary arterial hypertension (PAH) is a severe and frequently fatal disease that is caused by narrowing of the distal pulmonary vascular circulation leading to elevated pulmonary arterial pressure, right heart failure and death. Although pulmonary vascular tone is increased, most of the increase in pulmonary vascular resistance is caused by remodelling of the distal pulmonary vasculature. This remodelling includes endothelial dysfunction, smooth muscle cell hyperplasia and hypertrophy, as well as adventitial fibroblast proliferation, myofibroblast differentiation, and extracellular matrix deposition.[1,2] The mechanisms responsible for these myriad changes are not well understood, but include endothelial apoptosis and the emergence of hyper-proliferative, apoptosis resistant endothelial cells (ECs) that display a metabolic switch to predominantly glycolytic pathways.[3] Atypical abundances of functionally distinct ECs have been extensively reported to precede muscularization of distal

* Corresponding author. Tel: +1 401 444 5331; fax: +1 401 444 5006, E-mail: olin_liang@brown.edu

pulmonary arterioles leading to increased vascular resistance.[4] Concomitant inflammation marked by the presence of mononuclear cell infiltrates in the perivascular areas around affected vessels is another common feature of PAH.[4]

The source of these defective ECs and the mechanisms responsible for their transition to a hyper-proliferative phenotype are unclear. However, a growing line of evidence suggests that bone marrow (BM)-derived endothelial progenitor cells (EPCs) may contribute. The precise definition of EPC continues to evolve, but in general EPC refers to a haematopoietic/endothelial precursor cell (haemangioblast), that is capable of differentiating into both haematopoietic cells and ECs,[5,6] In postnatal life to adulthood, these haemangioblasts are readily identifiable in the BM in a small subpopulation of CD34+ haematopoietic stem cells (HSCs) that also demonstrate selective expression of CD133. Recent studies have shown that CD34+ CD133+ progenitors are increased in the plasma, BM and lungs of PAH patients compared with controls and that plasma levels of these cells correlate with severity of PAH. Farha et al. recently reported that CD34+ 133+ cells from PAH patients have greater proliferative capacity than circulating progenitors of healthy controls. They also showed that non-affected family members of patients with familial PAH displayed elevated circulating concentrations of CD34+ CD133+ cells, which were comparable with their affected relatives with PAH. Non-affected family members also had significant increase in marrow fibrosis compared with healthy unrelated controls. The investigators hypothesized that a subclinical myeloproliferative process is intrinsic to PAH, and that these myeloid abnormalities promote the pathologic vascular remodelling in the lung.[7] This hypothesis is further supported in a follow-up study in which mice transplanted with BM-derived CD133+ progenitor cells from patients with PAH developed pulmonary hypertension (PH).[8] Furthermore, marked infiltration of c-kit+ haematopoietic progenitor cells, especially in the perivascular compartment of remodelled arteries of idiopathic PAH patients has been reported[9] and therapeutic targeting of c-kit+ cells prevents hypoxia-induced PAH in mice.[10]

In adult mammals, including humans, blood cells arise from multilineage HSCs in the BM and thymus.[11] However, during embryonic development, haematopoiesis begins in the yolk sac from an endothelium with haemogenic properties, known as the haemogenic endothelium, first identified in the 1900s based on microscopic observations of developing embryos.[12–14] Later, Murray *et al.*[15] referred to the same cells as 'haemangioblasts' suggesting both endothelial and blood cells develop from them. Studies with murine embryos confirm findings in the haemangioblasts as a common precursor for endothelial and haematopoietic cells.[16] It is now believed that HSCs responsible for the generation of all blood cell types can arise from the haemogenic endothelium,[17,18] a hypothesis that is supported by recent time-lapse imaging experiments that visualized the transition of endothelium into blood in real-time, both *in vitro*[19] and *in/ex vivo*.[20–22] The process of ECs taking on a haematopoietic fate has been termed endothelial-to-haematopoietic transition (EHT), and is regulated by a specific set of transcription factors, such as Fli1, Scl/Tal1, Lmo2, Runx1, GATA1, GATA2.[23–26] Whether haemogenic ECs exist in adulthood and generate HSCs is currently unknown. Embryonic lineage-tracing studies, which label haemogenic ECs before definitive haematopoiesis and follow their progenies through adulthood, demonstrate that, although embryonic HSCs remain functional in adulthood, they do not account for all haematopoietic cells generated postnatally.[18]

In this study, we hypothesize that BM-derived EPCs acquire a haematopoietic phenotype via EHT which then lead to the vascular pathology in experimental PH. We demonstrate that during PH development in mice, EPCs mobilize from BM into the circulation, and these EPCs have haematopoietic properties and can be found in the remodelled pulmonary vasculature. Inhibition of EHT by blocking Runx1, one of the key transcription factors responsible for EHT, prevented disease progression in both Sugen/hypoxia (Su/Hx)- and monocrotaline (MCT)-induced PH mouse models. Furthermore, we found high levels of Runx1 expression in circulating CD34+ CD133+ EPCs isolated from peripheral blood of PH patients, supporting the clinical relevance of our proposed mechanism of EHT.

2. Methods

2.1 Mouse strains and procedures

Mice with endothelial specific expression of Cre recombinase (VE-cadherin-cre[27]), Rosa26-ZsGreen reporter mice, CD45.1 mice and C57BL/6 J mice were purchased from The Jackson Laboratory (Bar Harbor, ME). Mice were 6- to 10-weeks old when used for experiments. Genotyping was carried out with primers and conditions as recommended by The Jackson Laboratory. For euthanasia, the mice were sacrificed via CO_2 asphyxia followed by cervical dislocation. All animal experiments were approved by the Rhode Island Hospital (RIH) IACUC, and were performed conform the NIH guidelines (Guide for the care and use of laboratory animals).

2.2 Su/Hx-induced and MCT-induced PH mouse models

Although debate over validity of different PH mouse models is still ongoing, we chose Su/Hx-induced and MCT-induced PH mouse models for this study.[28–30] The Su/Hx-PH protocol consisted of 3 weekly s.c. injections of the Sugen VEGF receptor-2 inhibitor SU5416 (Tocris) at 20 mg/kg in 100 µl DMSO or vehicle alone.[31] During the 3-week SU5416 treatment, mice were exposed to hypoxia (8.5% O_2) or normoxia (Nx) for 3 weeks. For the MCT-induced PH mouse model, cohorts of mice received weekly subcutaneous injections of MCT (60 mg/kg, Sigma) resuspended in 100 µl of saline or 100 µl of saline only (vehicle) for 4 weeks. Mice were sacrificed 1 week after the last MCT injection. Development of PH was determined by measurement of right ventricular systolic pressure (RVSP), right ventricular (RV) hypertrophy (i.e. Fulton's index) and pulmonary vascular remodelling (i.e. vessel muscularization and wall thickness index). To measure RVSP, mice were anaesthetized via intra-peritoneal injection with ketamine (100 mg/kg) and xylazine (10 mg/kg). RVSP was measured through a trans-thoracic route with a Millar catheter transducer PVR-1030 (ADInstruments Inc., Colorado Springs, CO) and data were collected and analysed using the LabChart software v8.1.3 (ADInstruments). The mice were then sacrificed via cervical dislocation and each perfused with 10% formalin solution. Tissues were dissected and lungs were paraffin embedded, sectioned and stained with haematoxylin & eosin (H&E). Images of H&E stained lung tissues were taken by using a Nikon Eclipse E800 microscope (Nikon Instruments Inc., Melville, NY) equipped with a camera and SPOT Advanced 4.7 software (Diagnostic Instruments Inc., Sterling Heights, MI). Pulmonary arteriole wall thickness index indicates pulmonary vascular remodelling and was calculated as follows: Wall thickness index = [area(ext)-area(int)]/area(-ext), where area(ext) represents the external and area(int) represents the internal area of each vessel of less than 100 µm in diameter. The NIH ImageJ programme was used to assess vessel areas. The Fulton's index indicates RV hypertrophy and was calculated as follows: RV weight/[left

ventricular (LV) + septum (S) weight]. In order to demonstrate muscularization of distal pulmonary arteriole vessel wall, immunostaining was performed using a rabbit polyclonal antibody against α-smooth muscle actin (α-SMA) (1: 100, ab5694, Abcam, Cambridge, MA). Slides were then incubated with the EnVision+ Dual Link System-HRP solution (Agilent Technologies, Santa Clara, CA) containing anti-rabbit immunoglobulins conjugated to peroxidase-labelled polymer. Following chromogenic development, the slides were counterstained with haematoxylin. Images of α-SMA staining were then taken. Quantification of vessel muscularization was determined by the ratio of muscularized vessels/total number of vessels with diameter <50 μm.

2.3 Lineage tracing in Su/Hx-induced PH mouse model

VE-cadherin-cre mice were crossbred with Rosa26-ZsGreen mice to generate VE-cadherin-cre; ZsGreen double transgenic mice. In order to determine the haematopoietic phenotype of the double transgenic mice in the PH model, VE-cadherin-cre; ZsGreen mice were subjected to Su/Hx treatment and 50 μl of peripheral blood samples were collected weekly by retro-orbital bleeding from each mouse. For anaesthesia during retro-orbital blood sampling, the mice were anaesthetized via intraperitoneal injection with ketamine (100 mg/kg) and xylazine (10 mg/kg). BM cells were obtained by spinning femurs and tibias with a table centrifuge. After red blood cell lysis using ACK lysing buffer (Thermo Fisher Scientific, Waltham, MA), following antibodies were added to determine haematopoietic cell lineage: APC-CD45 (pan haematopoietic cells), PE-Gr-1 (myeloid cells), APC-Cy7-B220 (B-cells), and PerCP-Cy5.5-CD3e (T-cells). Dead cells were excluded by DAPI staining. These fluorophore labelled anti-mouse antibodies were purchased from BD Biosciences (San Jose, CA), eBioscience (Thermo Fisher Scientific, Waltham, MA) or Biolegend (San Diego, CA). Fluorescence-activated cell sorting (FACS) analyses were performed on a BD LSR II flow cytometer (BD Biosciences) and flow cytometry data were analysed using FlowJo software version 7.6.5 (FlowJo, LLC, Ashland, OR).

2.4 Immunofluorescence confocal imaging

Frozen sections of Nx and Su/Hx lungs of the VE-cadherin-cre; ZsGreen mice were stained with a goat anti-mouse c-kit antibody (AF1356, R&D Systems, Minneapolis, MN) at 15 μg/ml at 4 °C overnight and horse anti-goat DyLight 594 (DI-3094, Vector Laboratories, Burlingame, CA) at 10 μg/ml. Slides were mounted with VECTASHIELD mounting medium with DAPI (H-1200, Vector Laboratories). Fluorescence images were taken with Nikon C1si confocal microscope and analysed with the EZ-C1 software Ver3.90 (Nikon).

2.5 Gene expression analysis of ZsGreen+ c-kit+ CD45− EPCs

To determine gene expression pattern of the ZsGreen+ c-kit+ CD45- EPCs, we purchased the mouse haematopoiesis RT^2 Profiler PCR Array (Qiagen, Germantown, MD), which allows simultaneous analysis of 84 key genes involved in maintenance, self-renewal and differentiation. The ZsGreen+ cells were FACS sorted by using a BD Influx after staining mouse BM cells with the following antibodies (Biolegend): APC anti-mouse CD45 antibody and Brilliant Violet 421 anti-mouse CD117 (c-kit) antibody. For comparison, we also isolated the haematopoietic stem and progenitor Lineage- Sca-1+ c-kit+ (LSK) cells by using the BD Influx after staining mouse BM cells with the following antibodies (Biolegend): Brilliant Violet 421 anti-mouse lineage cocktail, Alexa Fluor 488 anti-mouse Ly-6 A/E (Sca-1) antibody and APC anti-mouse CD117 (c-kit) antibody. Next, total RNA was prepared from the freshly isolated cells immediately after sorting. Each cDNA was synthesized and mixed with RT^2 SYBR Green qPCR mastermix (Qiagen), and then divided equal volumes to each well of 96-well format array plate. Real time PCR was performed using CFX 96 Real Time System (Bio-Rad, Hercules, CA). The Ct values for all wells were exported to a Microsoft Excel spreadsheet for use with the PCR Array Data Analysis software [www.SABiosciences.com/pcrarraydataanalysis.php (25 August 2017, date last accessed)] according to the manufacturer's instruction. Gene expression level relative to that of the housekeeping gene GAPDH was calculated. A heat map was also generated by fold change that represents relative mRNA expression for ZsGreen+ c-kit+ CD45- EPCs compared with the LSK cells.

2.6 Transplantation of ZsGreen+ c-kit+ CD45− EPCs

For *in vivo* transplantation, 6- to 8-weeks old CD45.1+ mice were used as transplant recipients to distinguish donor-derived CD45.2+ haematopoietic cells from endogenous CD45.1+ haematopoietic cells. Isolated BM-derived ZsGreen+ c-kit+ CD45- EPCs (3×10^3 cells) combined with 3×10^5 CD45.1+ mouse BM cells were injected into lethally irradiated (twice 5 Gy 3 h apart) CD45.1+ recipient mice. After 4, 8, 12, and 16 weeks, peripheral blood samples (50 μl) from each recipient mouse were collected. Haematopoietic cell lineage FACS analysis was performed using the following antibodies (Biolegend): PE-CD45.1 (recipient haematopoietic cells), APC-CD45.2 (donor haematopoietic cells), PE-Cy7-Gr-1 (myeloid cells), APC-Cy7-B220 (B cells), and PE-Cy5-CD3e (T cells).

2.7 Runx1 inhibition *in vivo*

One week after Su/Hx-PH induction in C57BL/6 J mice or in the VE-cadherin-cre; ZsGreen mice, specific CBFβ-Runx1 inhibitor Ro5-3335[32] (EMD Millipore, Billerica, MA) was administered s.c. every other day at 50 mg/kg. Alleviation of PH was evaluated in inhibitor treated mice compared with vehicle injected control mice. The numbers of ZsGreen+ CD45+ cells in the peripheral blood of the VE-cadherin-cre; ZsGreen mice were analysed to determine whether Runx1 inhibition prevents potential EHT and PH progression. The numbers of ZsGreen+ c-kit+ CD45- EPCs in the BM of the double transgenic mice were also measured by using flow cytometry to determine whether Ro5-3335 intervention inhibits their egression.

2.8 Isolation of circulating CD34+ CD133+ EPCs from PH patients

Peripheral blood samples (12 ml each) were collected from healthy controls and from patients with PH who were undergoing right heart catheterization at the RIH Pulmonary Hypertension Center as part of their routine clinical evaluation. PH and PAH were defined according to consensus criteria using standard haemodynamic definitions.[33–34] All blood samples were obtained with local ethics committee approval (RIH IRB 257464, 021911, and 215915) and informed written consent. The investigation conformed to the principles outlined in the Declaration of Helsinki. We have established a flow cytometry protocol to sort CD45-CD14- CD34+ CD133+ EPCs from peripheral blood of patients and healthy controls. After red blood cell lysis, cells were stained with the following antibodies (Miltenyi, Auburn, CA) to deplete haematopoietic cells and enrich EPCs: CD45-Brilliant Violet 421, CD14-Brilliant Violet

421, CD34-Alexa Fluor 488, CD133-APC and VEGFR2-PE. DAPI was used to exclude dead cells. Human CD34+ CD133+ EPCs were collected by using a BD Influx cell sorter (BD Biosciences).

2.9 Quantitative RT-PCR of Runx1 expression

Total RNA was purified from patient and healthy control EPCs by using RNeasy Mini kit (Qiagen). First-strand cDNA was synthesized by using Super Script III kit (Invitrogen, Carlsbad, CA) from 1 μg total RNA according to the manufacturer's instructions. The sense and antisense primers (Integrated DNA Technologies, Coralville, IA) were as follows; human Runx1 (5′—ACC ACT CCA CTG CCT TTA AC—3′ and 5′—GAG AGT CGA CTG GAA AGT TCT G—3′); human GAPDH (5'—GTC AAC GGA TTT GGT CGT ATT G—3′ and 5′—TGG AAG ATG GTG ATG GGA TTT—3′). For quantitative analysis of gene expression, real-time PCR was performed by using SYBR Green I Master Mix on a CFX 96 Real-Time PCR Detection System (Bio-Rad). GAPDH expression was assessed as an internal reference for quantification. Relative gene expression level was expressed by the fold increase over internal control samples. Every real-time PCR was performed in triplicates.

2.10 Statistical analysis

Data are shown as the mean values ± S.E.M. The significance of difference was calculated with unpaired two-tailed Student's *t*-test or one-way ANOVA when comparing more than two groups by using GraphPad Prism version 6.03 (GraphPad Software, Inc., La Jolla, CA). *P* values < 0.05 were considered to be statistically significant.

3. Results

3.1 Assessment of the Su/Hx-induced PH mouse model

We used wild-type C57BL/6 J mice to establish the Su/Hx-PH mouse model by injecting a VEGFR2 inhibitor SU5416 once weekly during 3 weeks of hypoxia (8.5% O_2) (*Figure 1A*). After 3 weeks, Su/Hx treated mice developed significantly elevated RVSP [18.70 ±1.14 mmHg for Nx control group, 18.83 ± 0.88 mmHg for Sugen/normoxia (Su/Nx) control group and 25.65 ± 2.86 mmHg for Su/Hx-PH group] (*Figure 1B*). Su/Hx treated mice also had RV hypertrophy as indicated by a significant increase in the Fulton's index (RV/LV + S) compared with Nx and Su/Nx mice (*Figure 1C*). Upon immunostaining of α-SMA in the lung sections, significantly increased muscularization of distal pulmonary arteriole (<50 μm in diameter) vessel wall was also determined in the Su/Hx-treated mice compared with Nx and Su/Nx mice (*Figure 1D–F*, see Supplementary material online, *Figure S1A* and *B*). In addition, morphometric analysis of pulmonary arterioles suggested that Su/Hx treated mice had significant pulmonary vascular remodelling compared with Nx controls (see Supplementary material online, *Figure S1C–E*). Thus, Su/Hx-induced PH model produced appreciable PH pathology in mice.

3.2 Lineage tracing of cells with endothelial origin during PH development

In order to track potential *in vivo* transformation of ECs during PH induction, we generated VE-cadherin-cre; ZsGreen double transgenic mice, in which all ECs and EPCs were permanently labelled with the fluorescence protein ZsGreen. As shown in the frozen lung sections of the double transgenic mice, both large vessels and small capillaries were labelled green while epithelial bronchiolar airways, as internal negative controls, were not labelled green (*Figure 2A*, see Supplementary material online, *Figure S2A* and *B*). In addition to the lung, genetic labelling of vascular ECs in the heart and femur was also apparent when compared with respective tissue in the parental Rosa26-ZsGreen mice (see Supplementary material online, *Figure S2C–F*). Immunostaining of von Willebrand factor (vWF) was also performed in lung sections of the VE-cadherin-cre; ZsGreen double transgenic mice, which exhibited similar staining pattern as previously published.[35] Confocal fluorescence microscopy image of pulmonary arterioles showed that the vessel lumen lining ECs were co-stained with ZsGreen and vWF (see Supplementary material online, *Figure S3*). These VE-cadherin-cre; ZsGreen double transgenic mice were then subjected to Su/Hx treatment to induce PH, and 50 μl of peripheral blood samples were taken weekly (*Figure 2B*). It is worth noting that the VE-cadherin promoter is active in a small fraction of the haemangioblasts during embryonic development.[27] Our analysis suggests that approximately 20–30% of peripheral blood cells of the double transgenic mice are already labelled by ZsGreen (Nx W0 in *Figure 2C* and *D*). However, the percentage of ZsGreen+ cells with haematopoietic features as defined by expression of CD45+ increased significantly in peripheral blood after 1 week of Su/Hx treatment. More strikingly, more than 80% of the newly differentiated ZsGreen+ CD45+ haematopoietic cells in the peripheral blood were Gr-1+ myeloid cells which was significantly higher than in Nx mice (*Figure 2C–E*). After 2 weeks of Su/Hx treatment, while the percentage of ZsGreen+ CD45+ cells in the peripheral blood remained significantly higher than that in the Nx mice, myeloid cell, B cell and T cell composition among the ZsGreen+ CD45+ cells in the peripheral blood was comparable to that of the Nx mice (*Figure 2C–E*). After 3 weeks of Su/Hx treatment, the levels of ZsGreen+ CD45+ cells, myeloid cells, B cells and T cells in the peripheral blood all returned to those of Nx mice (*Figure 2C–E*). These results suggest that cells of endothelial origin have transformed into haematopoietic cells with myeloid propensity during PH development.

3.3 Egression of EPCs from the BM and their detection in the lung of PH mice

In comparison with the parental Rosa26-ZsGreen mice (*Figure 3A* and see Supplementary material online, *Figure S2E*), *in vivo* labelling of BM cells with endothelial origin in the double transgenic mice is shown in *Figure 3B* and see Supplementary material online, *Figure S2F*. The percentage of ZsGreen+ CD45+ cells in the BM remained constant during the 3 weeks of Su/Hx treatment, which were comparable to that of Nx mice (*Figure 3C* and *D*). Next, based on the postulation that ZsGreen+, i.e. activation of VE-cadherin promoter, represents endothelial origin, c-kit+ labels progenitor cells and CD45- indicates non-haematopoietic,[6,36,37] we used the combination ZsGreen+ c-kit+ CD45- to identify putative EPCs in the mouse BM. Intriguingly, the percentage of ZsGreen+ c-kit+ CD45- EPCs decreased dramatically in a time-dependent manner following Su/Hx treatment (*Figure 3E*). Furthermore, by using immunofluorescence staining and confocal microscopy we could identify a significant number of both ZsGreen+ c-kit+ cells and ZsGreen- c-kit+ cells (indicated by arrows and arrow heads, respectively, in *Figure 4A* and see Supplementary material online, *Figure S4A*) in the Su/Hx mouse lungs, whereas no c-kit+ cells were detected in the Nx mouse lungs (*Figure 4B* and see Supplementary material online, *Figure S4B*).

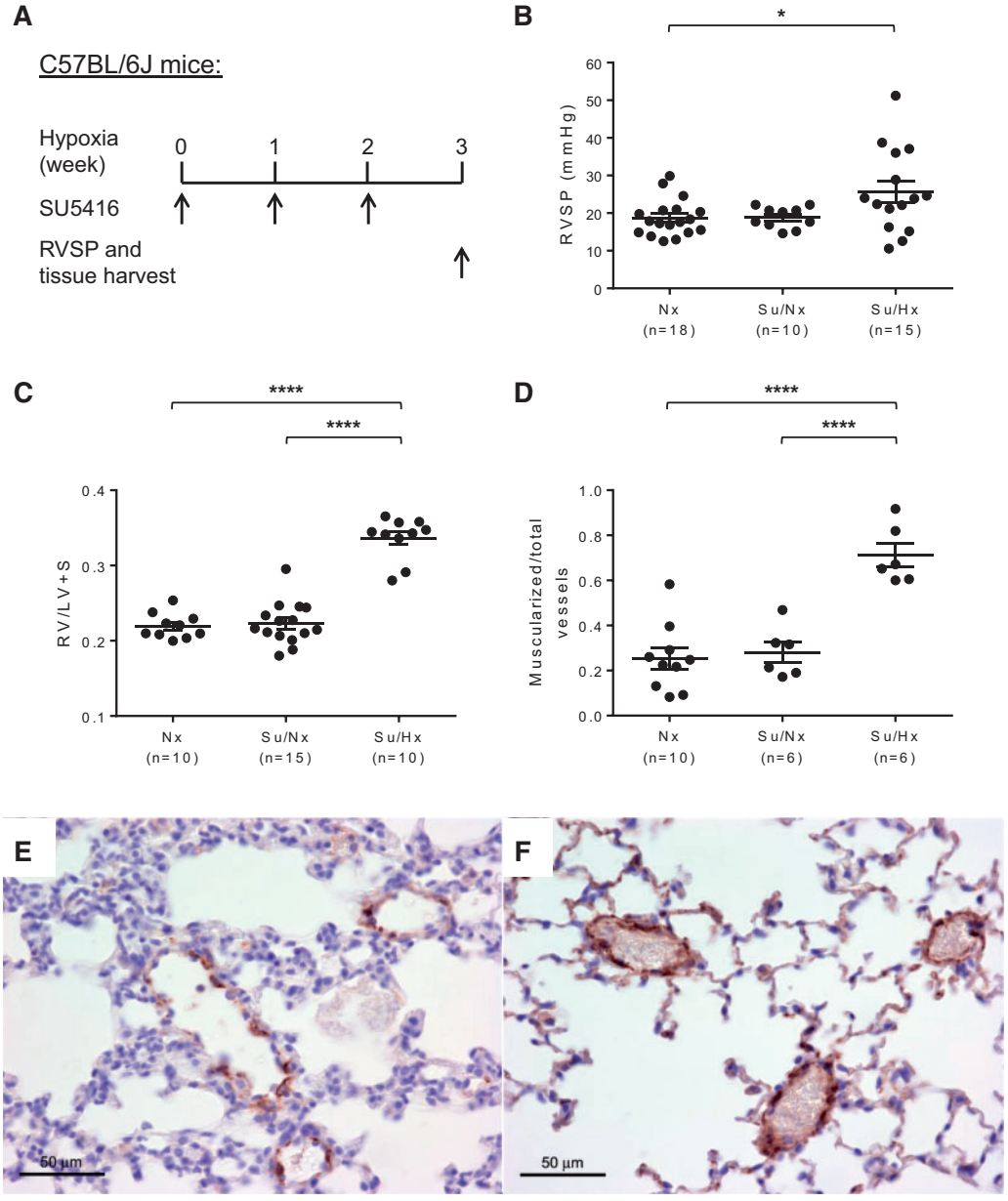

Figure 1 Su/Hx-induced PH model in mice. (*A*) Schematic of the experimental design using a combination of SU5416 and hypoxia treatment to induce PH in C57BL/6J mice. RVSP was measured and tissues were collected after 3 weeks of Su/Hx treatment. (*B*) Significantly elevated RVSP developed in Su/Hx mice ($n = 15$) compared with normoxia controls (Nx, $n = 18$). Sugen/normoxia control mice (Su/Nx, $n = 10$) were also included which had similar RVSP as the Nx mice. (*C*) Fulton's index (RV/LV+ S) was calculated to indicate the development of RV hypertrophy in Su/Hx mice ($n = 10$). Nx ($n = 10$) and Su/Nx ($n = 15$) control groups were also included and had similar Fulton's Index. Vessel wall muscularization of distal pulmonary arteriole (<50 µm in diameter) in Nx mice ($n = 10$), Su/Nx mice ($n = 6$) and Su/Hx mice ($n = 6$) was quantified based on immunostaining of α-SMA (*D*). Representative immunostaining images show increased expression of α-SMA (brown colour) in the distal pulmonary arteriole vessel walls of Su/Hx mice (*F*) compared with Nx controls (*E*). Original magnification 400×. Data in (*B–D*) are mean ± S.E.M. *$P < 0.05$, ****$P < 0.0001$, ordinary one-way ANOVA with multiple comparisons.

3.4 BM cells depleted of EPCs are unable to transfer PH pathology to recipient mice

A recent study suggests that BM cells may play a key role in PH pathogenesis and that the transplanted BM cells from *Bmpr2* mutant mice were able to drive the lung phenotype in a myeloablative transplant model.[38] We sought to test if BM cells from Su/Hx mice were able to cause PH pathology in transplant recipient mice. Total BM cells from Su/Hx treated mice were transplanted into lethally irradiated mice. RV hypertrophy of the recipient mice was assessed 4 weeks post-transplantation. The results showed that BM cells depleted of EPCs were unable to transfer PH pathology to recipient mice (see Supplementary material online, *Figure S5*).

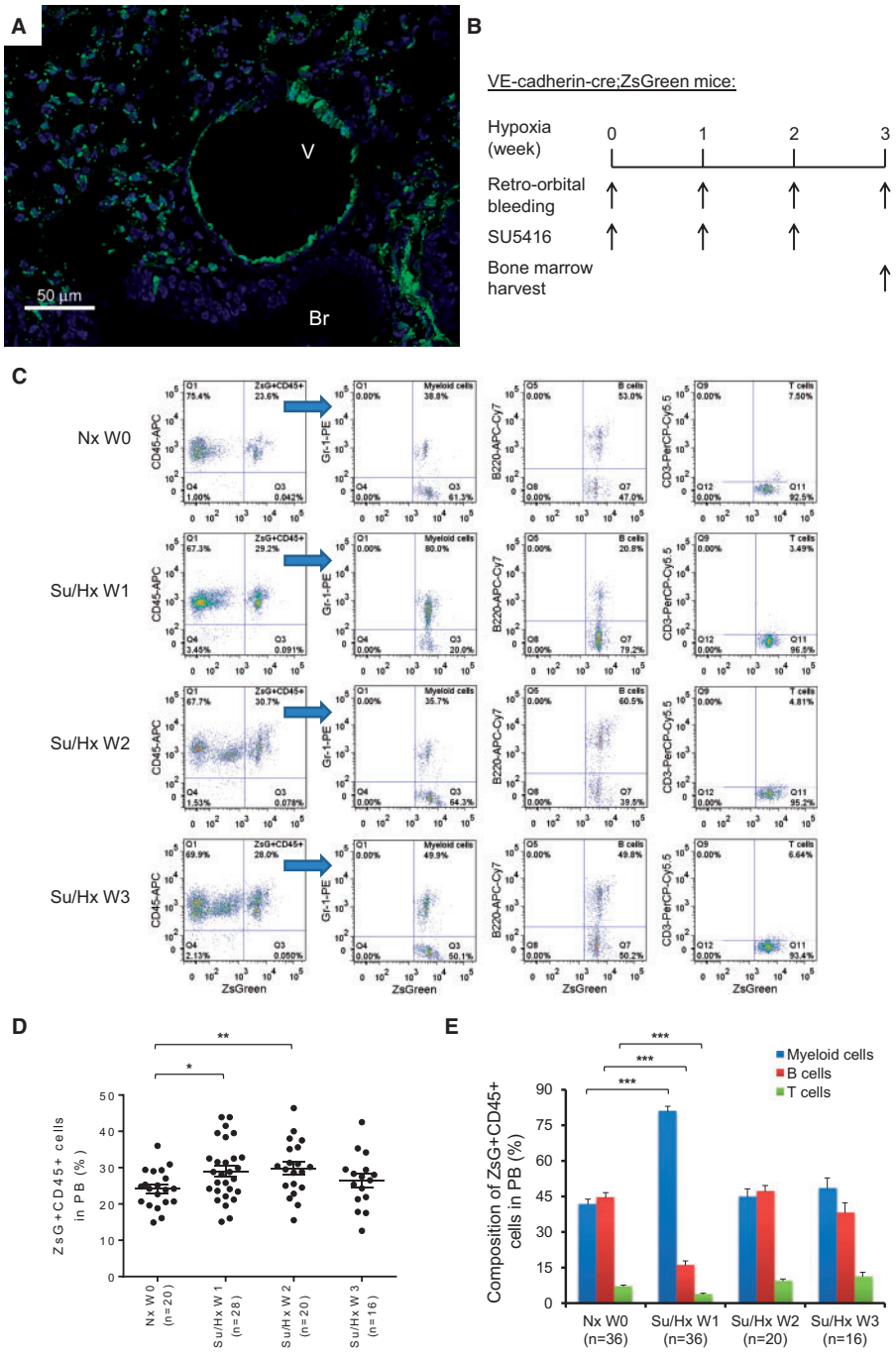

Figure 2 Myeloid skewed EHT during PH development. (*A*) Confocal fluorescence microscopy image of a frozen lung section of the VE-cadherin-cre; ZsGreen double transgenic mice (original magnification 400×). Green, fluorescence protein ZsGreen labelling of cells of endothelial origin; Blue, DAPI counterstaining of nuclei. Br, Bronchiole; V, Vessel. (*B*) Schematic of lineage tracing experimental design using VE-cadherin-cre; ZsGreen double transgenic mice in the Su/Hx-induced PH model. Mouse blood samples (50 µl) were collected at indicated time points and mouse BM was harvested at the end of the experiments. (*C–E*) The percentage of ZsGreen+ CD45+ haematopoietic cells, ZsGreen+ CD45+ cell-derived Gr-1+ myeloid cells, ZsGreen+ CD45+ cell-derived B220+ B cells and ZsGreen+ CD45+ cell-derived CD3+ T cells in the peripheral blood of the double transgenic mice are shown before Su/Hx treatment (Nx W0), 1 week after Su/Hx treatment (Su/Hx W1), 2 weeks after Su/Hx treatment (Su/Hx W2) and 3 weeks after Su/Hx treatment (Su/Hx W3). (*C*) Representative flow cytometry analysis plots are shown. (*D*) The percentage of ZsGreen+ CD45+ haematopoietic cells in mouse peripheral blood after 1 week (Su/Hx W1, $n = 28$) and 2 weeks (Su/Hx W2, $n = 20$) of Su/Hx treatment increased significantly compared with before Su/Hx treatment (Nx W0, $n = 20$). The percentage of ZsGreen+ CD45+ cells normalized after 3 weeks of Su/Hx treatment (Su/Hx W3, $n = 16$). (*E*) Significant myelopoiesis could be detected in mice 1-week post-Su/Hx treatment (Su/Hx 1 W, $n = 36$) compared with Nx W0 ($n = 36$). The blood cell composition normalized after 2 weeks (Su/Hx W2, $n = 20$) and 3 weeks (Su/Hx W3, $n = 16$) of Su/Hx treatment. Data in (*D*) and (*E*) are mean ± SEM. $^{*}P < 0.05$, $^{**}P < 0.01$, $^{***}P < 0.001$, unpaired two-tailed *t*-test.

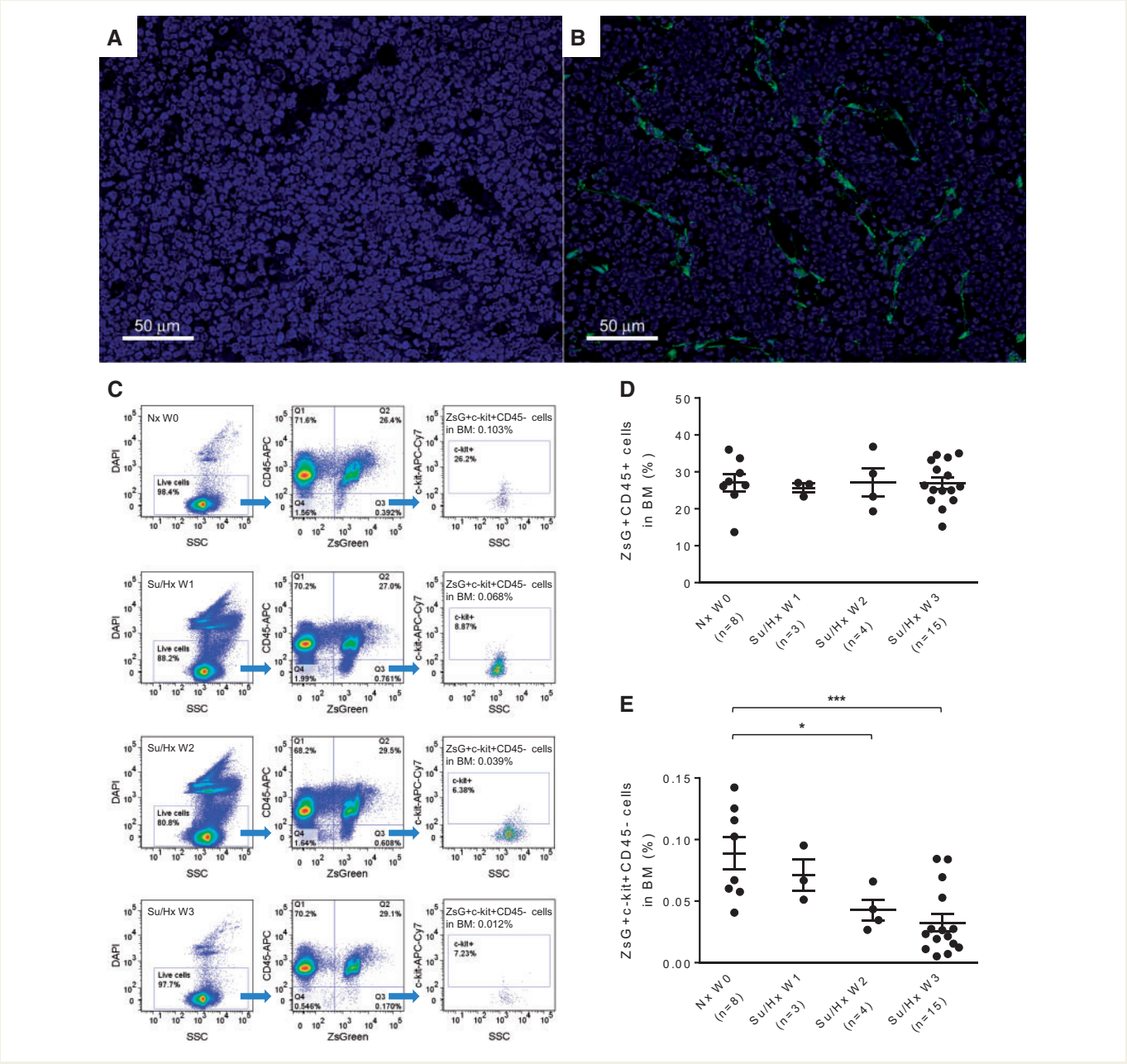

Figure 3 Su/Hx treatment of mice promotes egress of ZsGreen+ progenitor cells from BM. Confocal fluorescence microscopy image of a frozen femoral section from the Rosa26-ZsGreen reporter mice (*A*), and from the VE-cadherin-cre; ZsGreen double transgenic mice (*B*). Original magnification 400×, Green: fluorescence protein ZsGreen labelling of cells of endothelial origin; Blue: DAPI counterstaining of nuclei. Su/Hx treatment of the double transgenic mice promotes egress of ZsGreen+ c-kit+ CD45- progenitor cells from BM. (*C*) Representative flow cytometry analysis plots of BM cells at Nx W0, Su/Hx W1, Su/Hx W2, and Su/Hx W3 are shown. (*D*) The percentage of ZsGreen+ CD45+ haematopoietic cells in the BM remained unchanged. (*E*) The percentage of ZsGreen+ c-kit+ CD45- progenitor cells in the BM decreased in a time dependent manner. For both (*D*) and (*E*): Nx W0, $n = 8$; Su/Hx W1, $n = 3$; Su/Hx W2, $n = 4$ and Su/Hx W3, $n = 15$. Data in (*D*) and (*E*) are mean ± SEM. $^{*}P < 0.05$, $^{***}P < 0.001$, unpaired two-tailed *t*-test.

3.5 The putative EPCs from BM are haemogenic with myeloid propensity

By using a BD Influx cell sorter, we isolated from mouse BM the ZsGreen+ c-kit+ CD45- EPCs for haematopoietic gene expression analysis (*Figure 5A*). The results were then compared with gene expression profile of the BM-derived LSK population which is enriched with HSCs[39] (*Figure 5B*). We found that all critical transcription factors for haematopoiesis were expressed by the ZsGreen+ c-kit+ CD45- cells, including Cbfb, GATA1, GATA2, Lmo2, Runx1, and Scl/Tal1[40] (*Figure 5C*). In addition to the transcription factors, key regulators and markers of haematopoiesis such as Nos2 and Vav1 were also expressed in the ZsGreen+ EPCs (*Figure 5C* and see Supplementary material online, *Table S1*). Notably, several genes involved in myeloid-erythroid lineage differentiation (Ahsp, GATA1 and Trim10) were expressed at a higher level in the ZsGreen+ EPCs than in the LSK cells, whereas most other

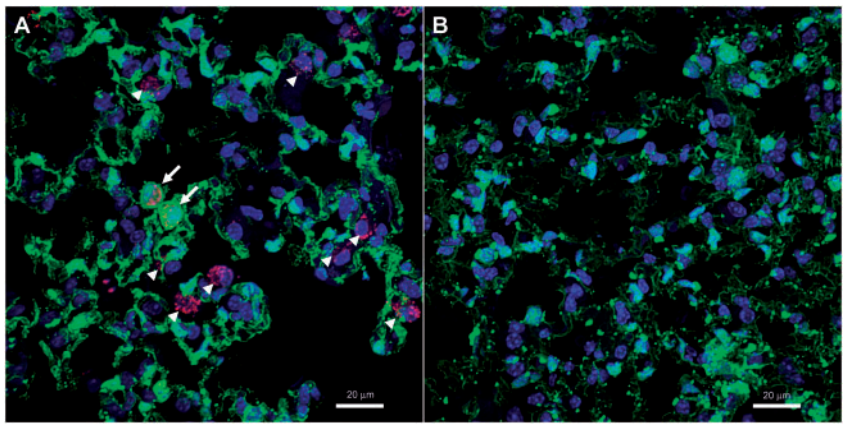

Figure 4 Emergence of EPCs in the lung of Su/Hx-treated mice. (*A*) Confocal immunofluorescence image of c-kit+ cells (magenta red) in a Su/Hx mouse lung. Frozen sections of Su/Hx lungs were stained with a goat anti-mouse c-kit antibody and horse anti-goat DyLight 594. Arrows: ZsGreen+ c-kit+ cells; arrow heads: ZsGreen- c-kit+ cells.. (*B*) No c-kit+ cells were detected in a Nx lung following the same immunofluorescence staining and confocal imaging. Original magnification 800×; Magenta red, Immunostaining of c-kit; Green, fluorescence protein ZsGreen labelling of cells of endothelial origin; Blue, DAPI counterstaining of nuclei. The experiments were performed three times and the images shown are representative.

genes were expressed on a comparable level between the two cells (*Figure 5D*). Next, we transplanted the ZsGreen+ c-kit+ CD45- EPCs into lethally irradiated mice. In syngeneic BM transplantation, C57BL/6 J mice with CD45.1 marker are often used as recipients and injected with haematopoietic stem and progenitor cells from congenic mice with CD45.2 marker. In this context, the donor or recipient cells can be easily identified by their allotypes of the leukocyte common antigen CD45. Donor-derived CD45.2+ haematopoietic cells were detected in the CD45.1 recipient mice 8 and 16 weeks post-transplantation (*Figure 5E*). Since the ratio of donor cell to CD45.1 radio-protective cell was 1: 100 (3×10^3 to 3×10^5), the maximal chimerism of donor-derived CD45.2 blood cells in the recipient would be 1%. Combined, these results strongly suggest that endothelium-derived progenitor cells from BM have the capability to undergo myeloid skewed haematopoiesis *in vivo*.

3.6 Runx1 inhibition blocks EHT *in vivo* and prevents egression of the EPCs from BM

Although transcription factors Fli1, Scl/Tal1, and Lmo2 are critical for earlier embryonic processes involved in endothelium specification from mesoderm, GATA2 is required for HSC generation and survival.[16,26,41] One transcription factor that has been a particularly useful marker of this developmental event in multiple species is Runx1, which is required for the EHT but not thereafter.[25,42] A recent high-throughput screening study revealed that a chemical compound Ro5-3335 was able to interrupt Runx1 binding to its heterodimeric partner CBF β, suppress Runx1-dependent haematopoiesis and inhibit leukemia in a mouse model.[32] We tested whether Ro5-3335 (50 mg/kg) or vehicle control could block Runx1-dependent EHT in the VE-cadherin-cre; ZsGreen double transgenic mice in Su/Hx-PH model (*Figure 6A*). One week into Su/Hx treatment, the percentage of ZsGreen+ CD45+ cells in the peripheral blood increased significantly (*Figure 6B* and *C*). However, when the mice were treated with Ro5-3335 every other day, the accumulation of the ZsGreen+ CD45+ cells in the peripheral blood diminished after 2 as well as 3 weeks of Su/Hx treatment (*Figure 6B* and *C*). Furthermore, the administration of Ro5-3335 significantly prevented egression of the ZsGreen+ c-kit+ CD45- EPCs from BM. After 3 weeks of Su/Hx treatment, the percentage of the ZsGreen+ c-kit+ CD45- EPCs in the BM of Su/Hx/Ro5 mice was significantly higher than that in Su/Hx mice, and had no difference compared with Nx mice (*Figure 6D* and *E*).

3.7 Runx1 inhibition prevents Su/Hx-induced PH in mice

To determine if Ro5-3335 inhibition of EHT resulted in amelioration of pulmonary hypertensive changes, we examined whether targeting Runx1 *in vivo* could prevent PH progression in mice (*Figure 7A*). After 3 weeks of Su/Hx treatment, RVSP and RV hypertrophy were significantly lower in mice treated with Ro5-3335 (Su/Hx/Ro5) than in mice without Ro5-3335 treatment (Su/Hx), and had no difference compared with Nx mice (*Figure 7B* and *C*). Immunostaining of α-SMA showed augmented muscularization in the distal pulmonary arteriole vessel walls of Su/Hx mice compared with Nx control mice and Ro5-3335 treated mice (*Figure 7D–G*, see Supplementary material online, *Figure S6A–C*). Morphometric analysis of pulmonary vessels also indicted that treatment with Ro5-3335 prevented pulmonary vascular remodelling. Pulmonary arteriole wall thickness index increased significantly in Su/Hx mice compared with Nx control mice and Ro5-3335 treated mice (see Supplementary material online, *Figure S6D–G*). These results suggest that specific Runx1 inhibition *in vivo* can prevent Su/Hx-induced PH in mice.

3.8 Runx1 inhibition alleviates MCT-induced PH in mice

In order to test if EHT may also contribute to the development of PH in other animal models of the disease, we applied Runx1 inhibitor Ro5-3335 in the MCT-induced PH mouse model (see Supplementary material online, *Figure S7A*). MCT treated mice developed significantly elevated RVSP, RV hypertrophy and vascular remodelling. Although injection of the Runx1 inhibitor Ro5-3335 did not reverse RVSP (see Supplementary material online, *Figure S7B*), the treatment reduced RV hypertrophy (see Supplementary material online, *Figure S7C*) as well as distal pulmonary vessel muscularization (see Supplementary material online, *Figure S7D–G*) in

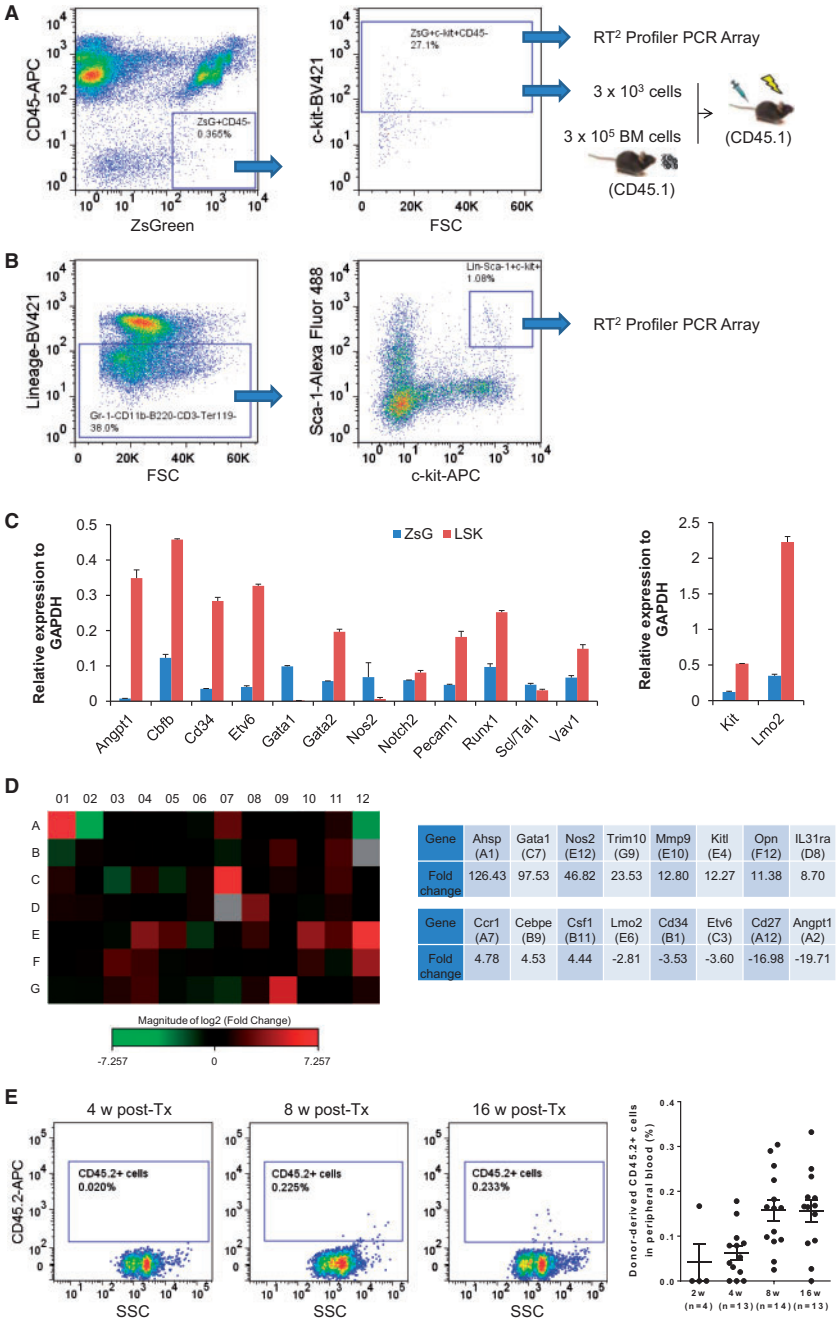

Figure 5 BM-derived ZsGreen+ c-kit+ CD45- progenitor cells are haemogenic. (*A*) FACS sorting strategy to isolate BM-derived ZsGreen+ c-kit+ CD45- EPCs from the VE-cadherin-cre; ZsGreen double transgenic mice ($n = 15$). Sorted cells were immediately used for haematopoietic gene expression analysis on a RT^2 Profiler PCR Array or for transplantation into lethally irradiated CD45.1 recipient mice ($n = 15$). The ratio between ZsGreen+ c-kit+ CD45- donor cells from CD45.2 mice (3×10^3) to radio-protective total BM cells from CD45.1 mice (3×10^5) was 1: 100 so that the maximal donor chimerism in the recipient mice would be 1%. (*B*) FACS sorting strategy to isolate BM-derived haematopoietic stem and progenitor enriched LSK cells from same age C57BL/6J mice ($n = 15$). Isolated LSK cells were immediately used for haematopoietic gene expression analysis on a RT^2 Profiler PCR Array. (*C*) Relative expression of key haematopoietic genes including transcription factors and markers by the ZsGreen+ c-kit+ CD45- putative haemogenic EPCs (ZsG, blue bars) and by the haematopoietic stem and progenitor enriched LSK cells (LSK, red bars). (*D*) Heat map of quantitative RT-PCR based gene array comparing 84 haematopoietic gene expression levels of the ZsG cells with the LSK cells. Red indicates up-regulation and green indicates down-regulation of the genes. Black suggests no significant changes in gene expression level. Grey indicates either undetectable or very low level of gene expression in both ZsG and LSK cells, and therefore no reasonable comparison can be made for those genes. Those genes that had most dramatic difference between these two cells are tabulated on the right of the heat map. The data shown in (*C*) and (*D*) are mean values of three experiments ($n = 15$ mice for ZsG cell isolation and $n = 15$ for LSK cell isolation). (*E*) Long-term engraftment and reconstitution capability of the BM-derived ZsGreen+ c-kit+ CD45- progenitor cells. Representative FACS analyses of chimerism in peripheral blood of the CD45.1 recipient mice are shown to indicate donor-derived CD45.2+ cells at 8 weeks ($n = 14$) and 16 weeks ($n = 13$) but not at 2 weeks ($n = 4$) or 4 weeks ($n = 13$) post-transplantation (Tx). Quantitative summary of all recipients are also shown on the right. Data in (*C*) and (*E*) are mean ± SEM.

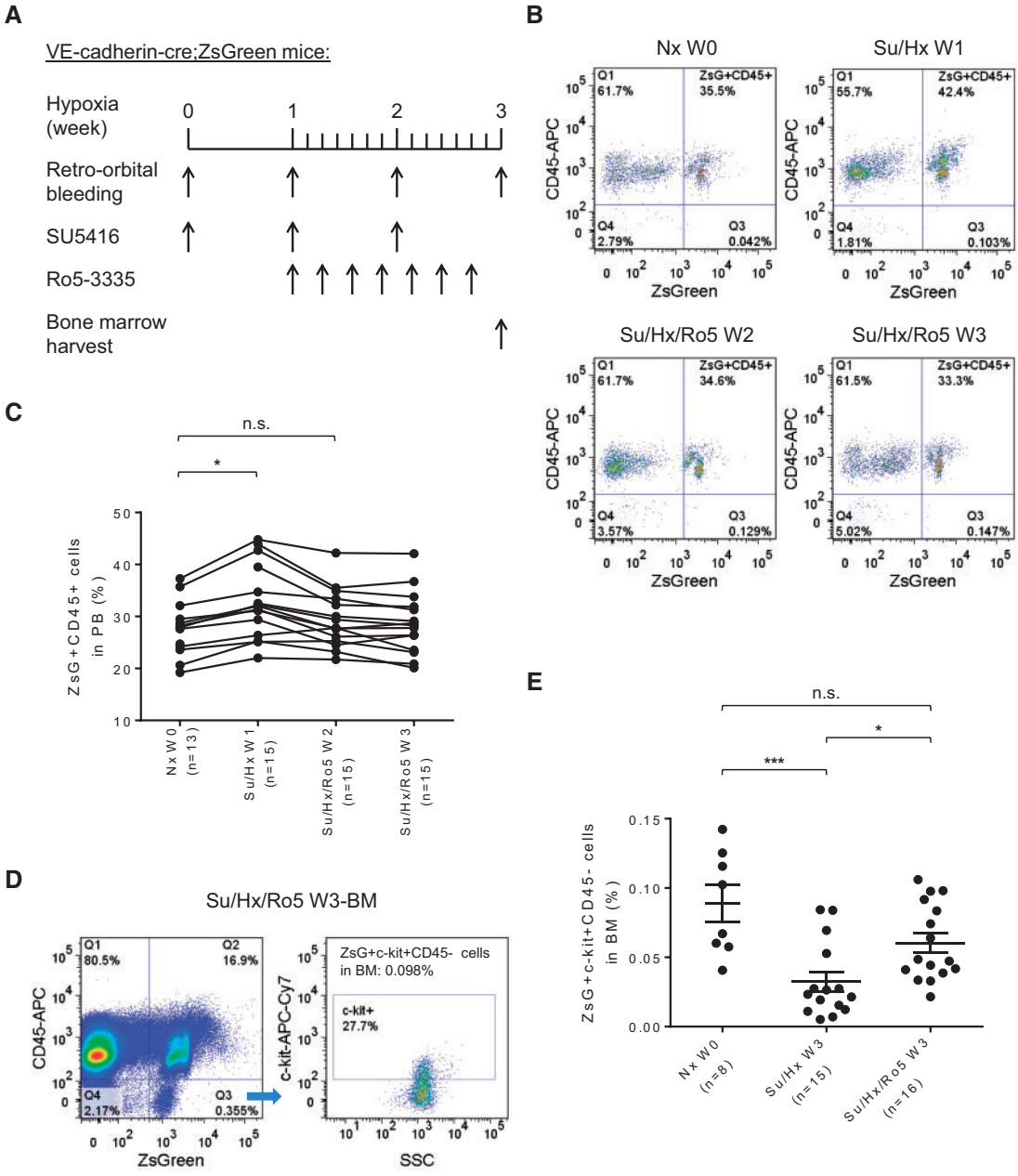

Figure 6 Specific Runx1 inhibition blocks EHT and prevents egress of the haemogenic progenitors from BM. (*A*) Schematic of the experimental design using specific Runx1 inhibitor Ro5-3335 in the Su/Hx-induced PH model with VE-cadherin-cre; ZsGreen double transgenic mice. Mouse blood samples (50 μl) were collected at indicated time points and mouse BM was harvested at the end of the experiment. Representative FACS plots (*B*) and summary analysis (*C*) showing the percentage of ZsGreen+ CD45+ haematopoietic cells before Su/Hx treatment (Nx W0, $n = 13$), 1 week after Su/Hx treatment (Su/Hx W1, $n = 15$), 2 weeks after Su/Hx and 1 week after Ro5-3335 treatment (Su/Hx/Ro5 W2, $n = 15$), and 3 weeks after Su/Hx and 2 weeks after Ro5-3335 treatment (Su/Hx/Ro5 W3, $n = 15$). Data in (*C*) are mean ± S.E.M. n.s., not significant; $^*P < 0.05$, unpaired two-tailed *t*-test. Representative FACS plots (*D*) and summary analysis (*E*) showing the percentage of ZsGreen+ c-kit+ CD45- progenitor cells in the BM with or without Ro5-3335 treatment in the Su/Hx-induced PH mice. Nx W0 ($n = 8$): before Su/Hx treatment; Su/Hx W3 ($n = 15$): 3weeks after Su/Hx treatment without Ro5-3335 treatment; Su/Hx/Ro5 W3 ($n = 16$): 3 weeks after Su/Hx and 2 weeks after Ro5-3335 treatment. Data in (*E*) are mean ± S.E.M. n.s., not significant; $^*P < 0.05$, $^{***}P < .001$, ordinary one-way ANOVA with multiple comparisons.

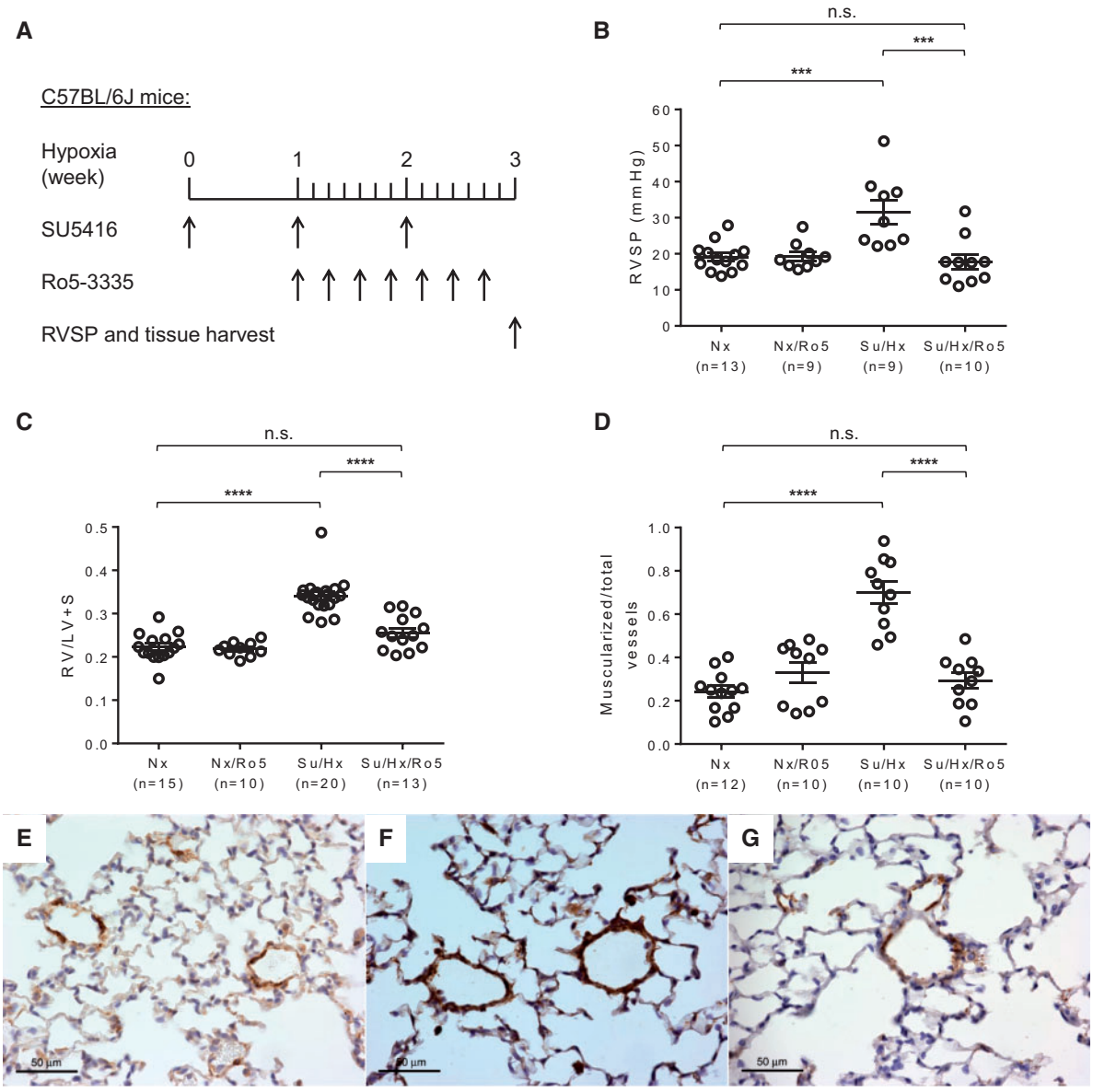

Figure 7 Specific Runx1 inhibition prevents the development of Su/Hx-induced PH in mice. (*A*) Schematic of the experimental design using specific Runx1 inhibitor Ro5-3335 in the Su/Hx-induced PH model with C57BL/6J mice. RVSP was measured and tissues were collected at the end of the experiment. (*B*) Runx1 inhibition prevented RVSP increase in mice treated with Su/Hx and Ro5-3335 (Su/Hx/Ro5, $n = 10$) compared with Su/Hx mice ($n = 9$). Nx ($n = 13$) and Nx/Ro5 ($n = 9$) control mice were also included. (*C*) Fulton's index (RV/LV+ S) was calculated to indicate the development of RV hypertrophy in Su/Hx mice ($n = 20$) and the absence of RV hypertrophy in Nx ($n = 15$), Nx/Ro5 ($n = 10$), and Su/Hx/Ro5 ($n = 13$) mice. (D, E, F and G) Vessel wall muscularization of distal pulmonary arteriole (<50 µm in diameter) in Nx mice ($n = 12$), Nx/Ro5 mice ($n = 10$), Su/Hx mice ($n = 10$) and Su/Hx/Ro5 mice ($n = 10$) was quantified based on immunostaining of α-SMA (*D*). Representative immunostaining images show increased expression of α-SMA (brown color) in the distal pulmonary arteriole vessel walls of Su/Hx mice (*F*) compared with Nx controls (*E*) and Su/Hx/Ro5 mice (*G*). Original magnification 400×. Data in (*B–D*) are mean ± S.E.M. n.s., not significant; ***$P < 0.001$, ****$P < 0.0001$, ordinary one-way ANOVA with multiple comparisons.

MCT+ Ro5-3335 group. These results suggest that specific Runx1 inhibition *in vivo* can also alleviate MCT-induced PH in mice.

3.9 High level expression of Runx1 in circulating EPCs isolated from PH patients

To further establish clinical relevance of our studies, we isolated CD34+ CD133+ EPCs from peripheral blood of patients diagnosed with PH. Patient characteristics, PH-subtype, haemodynamics (either at baseline or during follow-up catheterization) and concurrent PAH treatments at the time of study enrollment and blood draw are included in see Supplementary material online, *Table S2*. Based on our flow cytometry analysis, these EPCs constitute about 0.01–0.05% of total peripheral blood cells and they were collected by using a BD Influx cell sorter. Given the small sample volume (12 ml peripheral blood from each patient), no CD34+ CD133+ VEGFR2+ cells were detected, as the

triple markers have also been used to identify human circulating EPCs [43] (see Supplementary material online, *Figure S8A–E*). Next, we performed quantitative RT-PCR to show that Runx1, the critical haematopoietic transcription factor required for EHT, was highly expressed in the circulating EPCs of PH patients (see Supplementary material online, *Figure S8F*). These data demonstrate that Runx1 expression is increased in EPCs from patients with PH and support our hypothesis that EHT may play a role in human disease.

4. Discussion

Current therapies for PAH produce modest improvements in pulmonary vascular resistance and functional capacity and are effective at delaying the time to clinical worsening, but none of the interventions are etiology-based. Further advances in treatments will require therapies that inhibit and reverse the underlying causes of the disease. Here, we sought to determine if inflammatory cells that have been implicated in induction of pulmonary vascular remodelling in PAH derive in part from EHT and if blocking EHT could prevent disease progression.

Although no currently available model recapitulates all the features of human PAH, we used the combination of VEGF receptor-2 antagonist SU5416 and hypoxia to induce PH in mice. This model causes a more profound and sustained PH phenotype than with hypoxia alone, and allows the use of genetically modified mice to delineate potential pathogenic mechanisms. In consideration of our hypothesis of EHT, the use of VEGFR-2 blocker is attractive because it could facilitate the generation of many hyper-proliferative and apoptosis-resistant ECs and EPCs that would serve as the source of EHT. Ciuclan et al. observed occluded pulmonary arterioles in mice immediately after 3 weeks of Su/Hx but did not quantify these lesions.[29] However, no angio-obliterative lesions were found in our Su/Hx-mice, which is in agreement with recent reports by other investigators.[28,44] In this study, 3 weeks of treatment with Su/Hx resulted in the development of appreciable PH pathology in mice as evidenced by a significant increase of RVSP as well as a >50% increase in pulmonary vascular muscularization and RV free wall mass.

During the development of PH in Su/Hx treated mice, we found a significant increase in circulating haematopoietic cells of endothelial origin as evidenced by the percentage increase in ZsGreen+ CD45+ cells in peripheral blood. At the same time we found no change in the percentage of the ZsGreen+ CD45+ haematopoietic cells in the BM, but did observe a marked reduction in the amount of ZsGreen+ c-kit+ CD45- EPCs in the BM. The appearance of these cells in distal pulmonary vessels suggests a mobilization of the EPCs from BM into the lung. Despite the exponential rise in EPC research, the phenotypic classification of EPCs remains elusive.[37] In this study, the ZsGreen+ c-kit+ CD45- cells FACS sorted from BM expressed in addition to VE-cadherin (CD144) and c-kit (CD117) also the EC markers CD34 and PECAM (CD31) but not haematopoietic marker CD45 or monocyte/macrophage marker CD14 as indicated by the gene array analysis. As such, these cells definitely have endothelial markers but lack markers of blood cells. Concomitantly, they express a number of key haematopoietic transcription factors and are capable of reconstituting lethally irradiated recipient mice. The fact that these ZsGreen+ c-kit+ CD45- CD14- cells are haemogenic endothelial in nature and are capable of differentiating into haematopoietic cell lineages strongly suggests that the *de novo* production of ZsGreen+ CD45+ haematopoietic cells in PH mice is a bona fide EHT. Next, we found that BM cells from Su/Hx mice depleted of EPCs were unable to cause PH in transplant recipient mice, which supports the notion that BM-derived EPCs play a critical role in the pathogenesis of Su/Hx-PH in mice. In a separate study, we showed that BM-derived EPCs from MCT-PH mice could induce PH in healthy mice, but BM cells depleted of EPCs could not.[45] Further investigation in which transplantation of peripheral blood-derived ZsGreen+ CD45+ cells from Su/Hx-PH mice is warranted to directly demonstrate if these cells can cause PH in transplant recipients.

We further showed that inhibition of EHT by administration of a specific Runx1 inhibitor Ro5-3335 prevented the rise in ZsGreen+ CD45+ haematopoietic cells in peripheral blood and the fall in ZsGreen+ ckit+ CD45- EPCs in BM during Su/Hx-induced PH. Despite Su/Hx treatment, Runx1 inhibition blocked the egress of endothelial-derived EPCs from BM, prevented the increase of RVSP, pulmonary vascular remodelling as well as the development of RV hypertrophy. The molecular mechanisms with which Runx1 inhibition prevents the egression of EPCs from the BM remains unclear, but it is possible that downstream signals in the EPCs required for their mobilization (e.g. expression of cytokine receptors) become absent or reduced. Further experiments are needed to compare gene expression profiles in pulmonary versus BM-derived ZsGreen+ c-kit+ CD45- EPCs. In addition, we also used another mouse model of PH to demonstrate efficacy of the Runx1 inhibitor Ro5-3335. The MCT-induced PH model in mice has been well-established and was used in our previous studies.[30, 46] Runx1 inhibition in this model of PH prevented RV hypertrophy and pulmonary vascular remodelling but not the increase of RVSP. We speculate that the timing and duration of the Runx1 inhibitor intervention may need further optimization to obtain best outcome. It is also possible that in addition to EHT other disease mechanisms are also important in the MCT-induced PH mouse model. Combined, these findings indicate that EHT-derived haematopoietic cells play a critical role in the development of disease in experimental PH.

The VE-cadherin-cre; ZsGreen double transgenic mice showed inherently a 20–30% penetration in the haematopoietic lineage. This means that the VE-cadherin promoter was activated in a number of blood cells derived from haemogenic ECs during embryonic development, making it difficult to distinguish haematopoietic cells derived from EHT associated with experimental PH. We reason that the percentage increase in ZsGreen+ CD45+ cells is the result of de novo haematopoietic differentiation via EHT rather than proliferation of existing ZsGreen+ CD45+ cells, since ZsGreen- CD45+ cells would have proliferated in the same rate as well. Nevertheless, we cannot exclude the possibility that ZsGreen+ CD45+ and ZsGreen- CD45+ cells may behave differently. To overcome this limitation and to enhance endothelial specificity in lineage tracing, further experiments using inducible VE-cadherin-creERT2; ZsGreen mice in Su/Hx-PH model are ongoing in our laboratory.

Inflammation has recently been implicated as an integral factor during HSC emergence from haemogenic endothelium.[47] In the lung, injury to the endothelium by environmental factors is thought to be one of the precipitating events in PAH. At the onset of PAH, neutrophils or other inflammatory signals may traverse into BM to invoke haemogenic EPCs and initiate EHT. Previous studies have suggested that HIF-1α-induced factors such as erythropoietin, hepatocyte growth factor, SCF or VEGF are released by pulmonary vascular ECs to stimulate mobilization of BM-derived EPCs.[48] These stimuli may activate EHT which in turn produces pro-angiogenic myeloid cells that home to the lung, causing perivascular inflammation and remodelling. At the molecular level, Lancrin et al. demonstrated that the transcription factor Scl/Tal1 is indispensable for the establishment of the haemogenic endothelium population,[49] whereas the core binding factor Runx1 is critical for generation of definitive

haematopoietic cells from haemogenic endothelium.[25] The regulatory regions of haematopoietic genes are known to be bound by Runx1, as well as a transcription factor complex composed of Scl/Tal1, Lmo2, GATA1, and GATA2, all of which have been implicated in EHT.[16,40,50] All of these transcription factors were found to be highly expressed by the ZsGreen+ c-kit+ CD45- EPCs isolated from mouse BM. The expression of c-kit is another distinguishing feature of haemogenic relative to non-haemogenic ECs.[36]

Failure to resolve inflammation and altered immune processes are thought to underlie the development of PAH.[51] Lung inflammation precedes vascular remodelling in experimental PH suggesting that altered immunity is a cause rather than a consequence of vascular disease.[52] Increasing data indicate that inflammatory and immune mechanisms contribute to pulmonary vascular disease and this may be reflected in mobilization of cells from the BM. Thus, cells such as lymphocytes, monocytes, macrophages, and dendritic cells accumulate in pulmonary vascular lesions and raised levels of inflammatory mediators occur in the lungs and circulation of PAH patients.[8,38,53] Recent studies suggested that pulmonary tertiary lymphoid tissues could be directing local immune phenomena.[54,55] It is plausible that EHT may contribute to the ectopic lymphoid follicles in the lung. Reduced BMPR2 expression, a common feature of PAH, induces GM-CSF translation[56] which may potentially exacerbate myeloid skewed EHT.

Based on our current findings, reducing the number of EPCs in the circulation and blocking EHT of these cells could provide a potential strategy to alleviate PAH. Since differentiation of blood cells from the haemogenic endothelium is critically dependent on Runx1 expression, and Runx1 is likely to become dispensable beyond the haemogenic endothelium stage, this combination would make Runx1 a desirable target for treating pulmonary vascular disease in patients without affecting other physiological processes. Indeed, we could show that Runx1 is highly expressed in the circulating EPCs of PH patients, which provides important evidence that our proposed mechanism of EHT in animal models of PH may also be valid in human disease. This signal was significant despite the inclusion of several patients with PH from left heart disease (combined pre- and post-capillary PH and pure pulmonary venous hypertension); evidence of EHT may be even more apparent in a population of untreated 'pure' PAH patients. Isolation of EPCs from a larger cohort of only PAH patients (four of the patients in the current sample) should be performed to confirm our findings. Further clinically relevant experiments are warranted to test the Runx1 inhibitor in Su/Hx/Nx-model in rats that develop severe PH accompanied by occlusive pulmonary arterial neointimal and plexiform lesions.[57]

In summary, data from this study suggest that during the development of PH, BM-derived EPCs mobilize into the circulation and eventually the pulmonary vasculature where they play a critical role through the process of a myeloid skewed EHT. Blocking this process by specific inhibition of Runx1, one of the key transcription factors responsible for EHT, not only prevents the mobilization of EPCs but prevents disease progression in mice with Su/Hx- and MCT-induced PH. Finally, EPCs isolated from the blood of patients with PH have increased expression of Runx1. Together, these findings suggest that EHT plays an important role in the pathogenesis of PAH and that the haematopoietic transcription factor Runx1 may be a novel therapeutic target to treat PAH.

Supplementary material

Supplementary material is available at *Cardiovascular Research* online.

Acknowledgements

We thank Dr James Padbury, Mark Dooner, Michael Del Tatto, Elaine Papa, Mandy Pereira, Ginny Hovenasian and Lelia Noble for their kind help.

Conflict of interest: none declared.

Funding

This work was supported in part by grants from the National Institutes of Health (R01 HL112860, R01 HL123965, P20 GM119943, P20 GM103652, P20 GM104937, P30 GM114750, T32 HL094300 and T32 HL116249), and the Rhode Island Foundation (Medical Research Fund Nr. 20144121).

References

1. Rabinovitch M. Molecular pathogenesis of pulmonary arterial hypertension. *J Clin Invest* 2012;**122**:4306–4313.
2. Yeager ME, Frid MG, Stenmark KR. Progenitor cells in pulmonary vascular remodeling. *Pulm Circ* 2011;**1**:3–16.
3. Sakao S, Tatsumi K, Voelkel NF. Endothelial cells and pulmonary arterial hypertension: apoptosis, proliferation, interaction and transdifferentiation. *Respir Res* 2009;**10**:95.
4. Tuder RM, Groves B, Badesch DB, Voelkel NF. Exuberant endothelial cell growth and elements of inflammation are present in plexiform lesions of pulmonary hypertension. *Am J Pathol* 1994;**144**:275–285.
5. Yoder MC. Editorial: early and late endothelial progenitor cells are miR-tually exclusive. *J Leukoc Biol* 2013;**93**:639–641.
6. Yoder MC. Endothelial progenitor cell: a blood cell by many other names may serve similar functions. *J Mol Med* 2013;**91**:285–295.
7. Farha S, Asosingh K, Xu W, Sharp J, George D, Comhair S, Park M, Tang WH, Loyd JE, Theil K, Tubbs R, Hsi E, Lichtin A, Erzurum SC. Hypoxia-inducible factors in human pulmonary arterial hypertension: a link to the intrinsic myeloid abnormalities. *Blood* 2011;**117**:3485–3493.
8. Asosingh K, Farha S, Lichtin A, Graham B, George D, Aldred M, Hazen SL, Loyd J, Tuder R, Erzurum SC. Pulmonary vascular disease in mice xenografted with human BM progenitors from patients with pulmonary arterial hypertension. *Blood* 2012;**120**:1218–1227.
9. Montani D, Perros F, Gambaryan N, Girerd B, Dorfmuller P, Price LC, Huertas A, Hammad H, Lambrecht B, Simonneau G, Launay JM, Cohen-Kaminsky S, Humbert M. C-kit-positive cells accumulate in remodeled vessels of idiopathic pulmonary arterial hypertension. *Am J Respir Crit Care Med* 2011;**184**:116–123.
10. Gambaryan N, Perros F, Montani D, Cohen-Kaminsky S, Mazmanian M, Renaud JF, Simonneau G, Lombet A, Humbert M. Targeting of c-kit+ haematopoietic progenitor cells prevents hypoxic pulmonary hypertension. *Eur Respir J* 2011;**37**:1392–1399.
11. Orkin SH, Zon LI. Hematopoiesis: an evolving paradigm for stem cell biology. *Cell* 2008;**132**:631–644.
12. Jordan HE. Evidence of hemogenic capacity of endothelium. *Anat Rec* 1916;**10**:417–420.
13. Emmel VE. The cell clusters in the dorsal aorta of mammalian embryos. *Am J Anat* 1916;**19**:401–421.
14. Sabin FR. Studies on the origin of blood vessels and of red corpuscles as seen in the living blastoderm of the chick during the second day of incubation. *Contrib Embryol* 1920;**9**:213–262.
15. Murray PDF. The development in vitro of the blood of the early chick embryo. *Proc R Soc Lond B* 1932;**111**:497–521.
16. Costa G, Kouskoff V, Lacaud G. Origin of blood cells and HSC production in the embryo. *Trends Immunol* 2012;**33**:215–223.
17. Hirschi KK. Hemogenic endothelium during development and beyond. *Blood* 2012;**119**:4823–4827.
18. Zovein AC, Hofmann JJ, Lynch M, French WJ, Turlo KA, Yang Y, Becker MS, Zanetta L, Dejana E, Gasson JC, Tallquist MD, Iruela-Arispe ML. Fate tracing reveals the endothelial origin of hematopoietic stem cells. *Cell Stem Cell* 2008;**3**:625–636.
19. Eilken HM, Nishikawa S, Schroeder T. Continuous single-cell imaging of blood generation from haemogenic endothelium. *Nature* 2009;**457**:896–900.
20. Kissa K, Herbomel P. Blood stem cells emerge from aortic endothelium by a novel type of cell transition. *Nature* 2010;**464**:112–115.
21. Bertrand JY, Chi NC, Santoso B, Teng S, Stainier DY, Traver D. Haematopoietic stem cells derive directly from aortic endothelium during development. *Nature* 2010;**464**:108–111.
22. Boisset JC, van Cappellen W, Andrieu-Soler C, Galjart N, Dzierzak E, Robin C. In vivo imaging of haematopoietic cells emerging from the mouse aortic endothelium. *Nature* 2010;**464**:116–120.
23. Marcelo KL, Goldie LC, Hirschi KK. Regulation of endothelial cell differentiation and specification. *Circ Res* 2013;**112**:1272–1287.

24. Park C, Kim TM, Malik AB. Transcriptional regulation of endothelial cell and vascular development. *Circ Res* 2013;**112**:1380–1400.
25. Chen MJ, Yokomizo T, Zeigler BM, Dzierzak E, Speck NA. Runx1 is required for the endothelial to haematopoietic cell transition but not thereafter. *Nature* 2009;**457**:887–891.
26. de Pater E, Kaimakis P, Vink CS, Yokomizo T, Yamada-Inagawa T, van der Linden R, Kartalaei PS, Camper SA, Speck N, Dzierzak E. Gata2 is required for HSC generation and survival. *J Exp Med* 2013;**210**:2843–2850.
27. Alva JA, Zovein AC, Monvoisin A, Murphy T, Salazar A, Harvey NL, Carmeliet P, Iruela-Arispe ML. VE-Cadherin-Cre-recombinase transgenic mouse: a tool for lineage analysis and gene deletion in endothelial cells. *Dev Dyn* 2006;**235**:759–767.
28. Vitali SH, Hansmann G, Rose C, Fernandez-Gonzalez A, Scheid A, Mitsialis SA, Kourembanas S. The Sugen 5416/hypoxia mouse model of pulmonary hypertension revisited: long-term follow-up. *Pulm Circ* 2014;**4**:619–629.
29. Ciuclan L, Bonneau O, Hussey M, Duggan N, Holmes AM, Good R, Stringer R, Jones P, Morrell NW, Jarai G, Walker C, Westwick J, Thomas M. A novel murine model of severe pulmonary arterial hypertension. *Am J Respir Crit Care Med* 2011;**184**:1171–1182.
30. Aliotta JM, Pereira M, Amaral A, Sorokina A, Igbinoba Z, Hasslinger A, El-Bizri R, Rounds SI, Quesenberry PJ, Klinger JR. Induction of pulmonary hypertensive changes by extracellular vesicles from monocrotaline-treated mice. *Cardiovasc Res* 2013;**100**:354–362.
31. Li L, McLoughlin P. Choice of vehicle in the SUGEN/Hypoxia model of pulmonary hypertension: Carboxymethylcellulose or Dimethyl Sulfoxide. *Am J Respir Crit Care Med* 2014;**189**:A3339.
32. Cunningham L, Finckbeiner S, Hyde RK, Southall N, Marugan J, Yedavalli VR, Dehdashti SJ, Reinhold WC, Alemu L, Zhao L, Yeh JR, Sood R, Pommier Y, Austin CP, Jeang KT, Zheng W, Liu P. Identification of benzodiazepine Ro5-3335 as an inhibitor of CBF leukemia through quantitative high throughput screen against RUNX1-CBFbeta interaction. *Proc Natl Acad Sci U S A* 2012;**109**:14592–14597.
33. Galie N, Humbert M, Vachiery JL, Gibbs S, Lang I, Torbicki A, Simonneau G, Peacock A, Vonk Noordegraaf A, Beghetti M, Ghofrani A, Gomez Sanchez MA, Hansmann G, Klepetko W, Lancellotti P, Matucci M, McDonagh T, Pierard LA, Trindade PT, Zompatori M, Hoeper M, Aboyans V, Vaz Carneiro A, Achenbach S, Agewall S, Allanore Y, Asteggiano R, Paolo Badano L, Albert Barbera J, Bouvaist H, Bueno H, Byrne RA, Carerj S, Castro G, Erol C, Falk V, Funck-Brentano C, Gorenflo M, Granton J, Iung B, Kiely DG, Kirchhof P, Kjellstrom B, Landmesser U, Lekakis J, Lionis C, Lip GY, Orfanos SE, Park MH, Piepoli MF, Ponikowski P, Revel MP, Rigau D, Rosenkranz S, Voller H, Luis Zamorano J. 2015 ESC/ERS Guidelines for the diagnosis and treatment of pulmonary hypertension: The Joint Task Force for the Diagnosis and Treatment of Pulmonary Hypertension of the European Society of Cardiology (ESC) and the European Respiratory Society (ERS): Endorsed by: Association for European Paediatric and Congenital Cardiology (AEPC), International Society for Heart and Lung Transplantation (ISHLT). *Eur Heart J* 2016;**37**:67–119.
34. Vachiery JL, Adir Y, Barbera JA, Champion H, Coghlan JG, Cottin V, De Marco T, Galie N, Ghio S, Gibbs JS, Martinez F, Semigran M, Simonneau G, Wells A, Seeger W. Pulmonary hypertension due to left heart diseases. *J Am Coll Cardiol* 2013;**62**:D100–D108.
35. Yamamoto K, de Waard V, Fearns C, Loskutoff DJ. Tissue distribution and regulation of murine von Willebrand factor gene expression in vivo. *Blood* 1998;**92**:2791–2801.
36. Gritz E, Hirschi KK. Specification and function of hemogenic endothelium during embryogenesis. *Cell Mol Life Sci* 2016;**73**:1547–1567.
37. Basile DP, Yoder MC. Circulating and tissue resident endothelial progenitor cells. *J Cell Physiol* 2014;**229**:10–16.
38. Yan L, Chen X, Talati M, Nunley BW, Gladson S, Blackwell T, Cogan J, Austin E, Wheeler F, Loyd J, West J, Hamid R. Bone marrow-derived cells contribute to pathogenesis of pulmonary arterial hypertension. *Am J Respir Crit Care Med* 2016;**193**:898–909.
39. Lin KK, Goodell MA. Detection of hematopoietic stem cells by flow cytometry. *Methods Cell Biol* 2011;**103**:21–30.
40. Wilkinson AC, Gottgens B. Transcriptional regulation of haematopoietic stem cells. *Adv Exp Med Biol* 2013;**786**:187–212.
41. Gao X, Johnson KD, Chang YI, Boyer ME, Dewey CN, Zhang J, Bresnick EH. Gata2 cis-element is required for hematopoietic stem cell generation in the mammalian embryo. *J Exp Med* 2013;**210**:2833–2842.
42. Lichtinger M, Ingram R, Hannah R, Muller D, Clarke D, Assi SA, Lie ALM, Noailles L, Vijayabaskar MS, Wu M, Tenen DG, Westhead DR, Kouskoff V, Lacaud G, Gottgens B, Bonifer C. RUNX1 reshapes the epigenetic landscape at the onset of haematopoiesis. *Embo J* 2012;**31**:4318–4333.
43. Yoder MC. Human endothelial progenitor cells. *Cold Spring Harb Perspect Med* 2012;**2**:a006692.
44. Gomez-Arroyo J, Saleem SJ, Mizuno S, Syed AA, Bogaard HJ, Abbate A, Taraseviciene-Stewart L, Sung Y, Kraskauskas D, Farkas D, Conrad DH, Nicolls MR, Voelkel NF. A brief overview of mouse models of pulmonary arterial hypertension: problems and prospects. *Am J Physiol Lung Cell Mol Physiol* 2012;**302**:L977–L991.
45. Aliotta JM, Pereira M, Dooner M, DelTatto M, Papa E, Wen S, Goldberg LR, Quesenberry PJ. Endothelial progenitor cells are the bone marrow cell population in mice with monocrotaline-induced pulmonary hypertension which induce pulmonary hypertension in healthy mice. *Blood* 2015;**126**:3455.
46. Aliotta JM, Pereira M, Wen S, Dooner MS, Del Tatto M, Papa E, Goldberg LR, Baird GL, Ventetuolo CE, Quesenberry PJ, Klinger JR. Exosomes induce and reverse monocrotaline-induced pulmonary hypertension in mice. *Cardiovasc Res* 2016;**110**:319–330.
47. Espin-Palazon R, Stachura DL, Campbell CA, Garcia-Moreno D, Del Cid N, Kim AD, Candel S, Meseguer J, Mulero V, Traver D. Proinflammatory signaling regulates hematopoietic stem cell emergence. *Cell* 2014;**159**:1070–1085.
48. Duong HT, Erzurum SC, Asosingh K. Pro-angiogenic hematopoietic progenitor cells and endothelial colony-forming cells in pathological angiogenesis of bronchial and pulmonary circulation. *Angiogenesis* 2011;**14**:411–422.
49. Lancrin C, Sroczynska P, Stephenson C, Allen T, Kouskoff V, Lacaud G. The haemangioblast generates haematopoietic cells through a haemogenic endothelium stage. *Nature* 2009;**457**:892–895.
50. Lancrin C, Sroczynska P, Serrano AG, Gandillet A, Ferreras C, Kouskoff V, Lacaud G. Blood cell generation from the hemangioblast. *J Mol Med* 2010;**88**:167–172.
51. Rabinovitch M, Guignabert C, Humbert M, Nicolls MR. Inflammation and immunity in the pathogenesis of pulmonary arterial hypertension. *Circ Res* 2014;**115**:165–175.
52. Tamosiuniene R, Tian W, Dhillon G, Wang L, Sung YK, Gera L, Patterson AJ, Agrawal R, Rabinovitch M, Ambler K, Long CS, Voelkel NF, Nicolls MR. Regulatory T cells limit vascular endothelial injury and prevent pulmonary hypertension. *Circ Res* 2011;**109**:867–879.
53. Popat U, Frost A, Liu E, May R, Bag R, Reddy V, Prchal JT. New onset of myelofibrosis in association with pulmonary arterial hypertension. *Ann Intern Med* 2005;**143**:466–467.
54. Perros F, Dorfmuller P, Montani D, Hammad H, Waelput W, Girerd B, Raymond N, Mercier O, Mussot S, Cohen-Kaminsky S, Humbert M, Lambrecht BN. Pulmonary lymphoid neogenesis in idiopathic pulmonary arterial hypertension. *Am J Respir Crit Care Med* 2012;**185**:311–321.
55. Colvin KL, Cripe PJ, Ivy DD, Stenmark KR, Yeager ME. Bronchus-associated lymphoid tissue in pulmonary hypertension produces pathologic autoantibodies. *Am J Respir Crit Care Med* 2013;**188**:1126–1136.
56. Sawada H, Saito T, Nickel NP, Alastalo T-P, Glotzbach JP, Chan R, Haghighat L, Fuchs G, Januszyk M, Cao A, Lai Y-J, Perez V. D J, Kim Y-M, Wang L, Chen P-I, Spiekerkoetter E, Mitani Y, Gurtner GC, Sarnow P, Rabinovitch M. Reduced BMPR2 expression induces GM-CSF translation and macrophage recruitment in humans and mice to exacerbate pulmonary hypertension. *J Exp Med* 2014;**211**:263–280.
57. Toba M, Alzoubi A, O'neill KD, Gairhe S, Matsumoto Y, Oshima K, Abe K, Oka M, McMurtry IF. Temporal hemodynamic and histological progression in Sugen5416/hypoxia/normoxia-exposed pulmonary arterial hypertensive rats. *Am J Physiol Heart Circ Physiol* 2014;**306**:H243–H250.